STRENGTHENING A PRESTRESSED CONCRETE SLAB BY EPOXY-BONDED FRP COMPOSITES AND SFRC OVERLAYER

Joaquim A. O. Barros[(1)] and José M. Sena Cruz[(2)]
Department of Civil Eng., School of Eng., University of Minho, Campus de Azurém, 4800-058 Guimarães, Portugal.
[(1)] barros@eng.uminho.pt, [(2)] jsena@eng.uminho.pt

Abstract

Laminates of carbon fibre reinforced polymer (CFRP), layer of steel fibre reinforced concrete (SFRC) and the simultaneous use of CFRP laminates and SFRC overlayer were the strengthening strategies analysed for increasing the load bearing capacity of a concrete slab. A numerical model developed for simulating these strengthening techniques is described and the results obtained are analysed.

Keywords: strengthening, carbon fibre reinforced polymer, steel fibre reinforced concrete

1 - Introduction

In a building with insufficient support conditions a textile machine placed on a concrete slab will be replaced by a new one much heavy. To enhance the deficient support conditions of the building, additional reinforced concrete frames supported on micro-piles were built nearest as possible of the slab supports, in order to disturb, as minimum as possible, the functionality of the warehouse underneath the slab (see scheme of Figure 1 and photos in Figure 2).

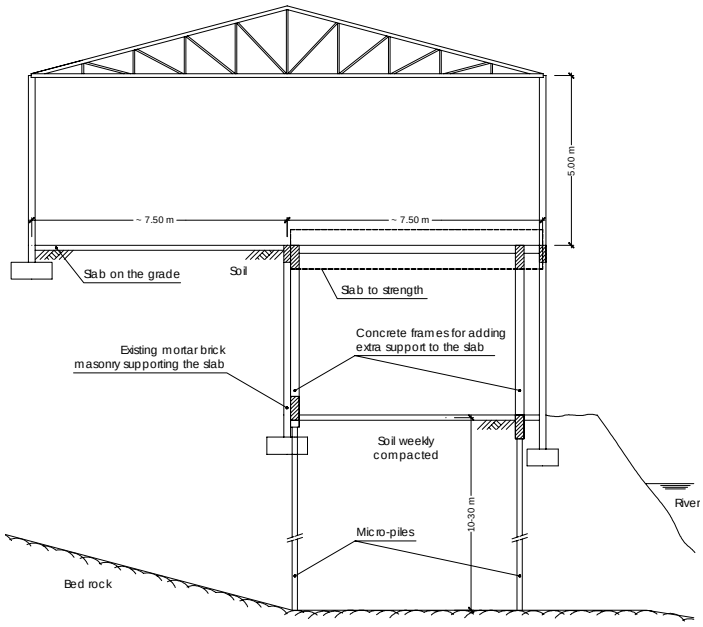

Figure 1 – Strategy for adding extra supports to the slab.

Figure 2 – Frames supporting the slab.

For increasing the slab load bearing capacity the three reinforcing techniques, schematically represented in Figure 3 were analysed: applying epoxy-bonded laminates of carbon fibre reinforced polymer (CFRP) [1]; using a top over-layer of steel fibre reinforced concrete (SFRC) [2]; combining the two last ones. The numerical model developed for designing the strengthening techniques applied on the slab will be described in the present work, and the results obtained will be analysed.

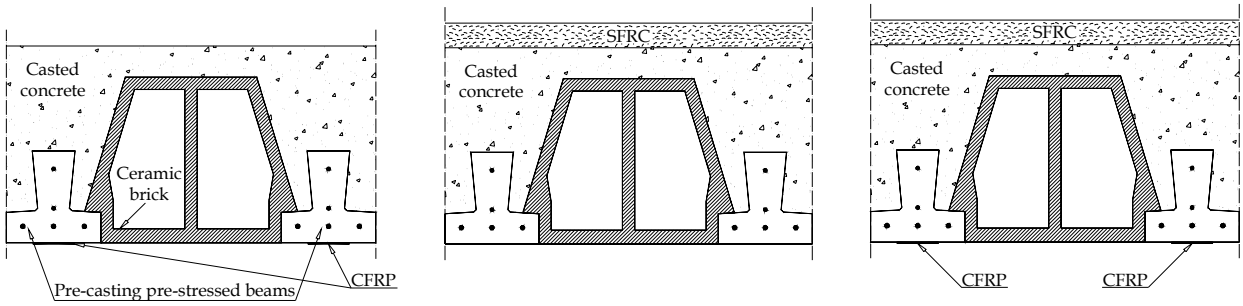

(a) (b) (c)

Figure 3 – Techniques for increasing the slab load bearing capacity: (a) using CFRP; (b) applying a top overlayer of SFRC; (c) using the two last strategies.

2 – Numerical model

2.1 – Introduction

The present model can be applied on a cross section of any shape and submitted to an axial force and two bending curvatures. The cross section can be composed of different concrete, steel and composite materials. To be useful for strengthening design, the model can simulate materials with a given initial strain and stress. The finite element mesh discretizing the cross section is dependent on the geometry and on the materials composing this cross section (see Figure 4). The moment-curvature relationships are obtained taking into account the material constitutive laws and the equilibrium and the kinematic equations. Appropriated constitutive laws simulate the monotonic and the cyclic behaviour of the aforementioned materials.

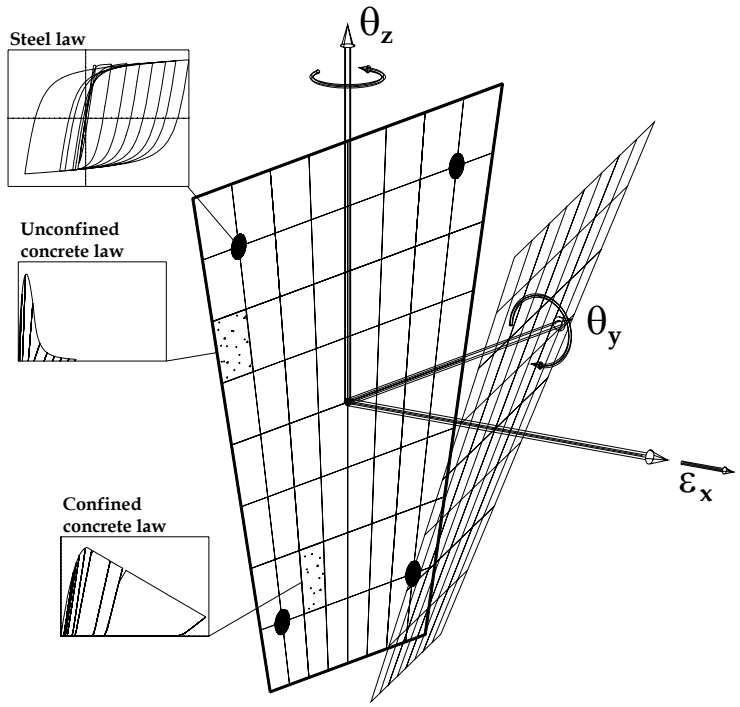

Figure 4 – Cross section model representation.

2.2 - Materials

Plain concrete (PC): The monotonic compression behaviour is simulated by the expressions proposed by the CEB-FIP Model Code [3]. The confinement provided by conventional stirrups or hoops is taken into account using the model developed by Scott et al [4]. The formulation proposed by Thompson and Park [5] was used for governing the unload-reload branches. Up to cracking, the PC tensile behaviour is simulated by the Young modulus and the axial tensile strength, whereas the post-cracking behaviour is modelled by the fracture parameters [6]. The tensile stiffness of the unload-reload branches of the cracked PC is considered constant and equal to the tensile stiffness of the uncracked PC.

Steel fibre reinforced concrete (SFRC): Previous work [6] has shown that the complete stress-strain expressions proposed for plain concrete cannot adequately fit the post-peak response of the fibre concrete. Based on experimental research, a new expression was proposed [6] that was implemented in the present model. The energy absorption capacity of the cracked concrete is the property most benefited by adding fibres to a concrete mix. This property can be evaluated from three points bending tests, determining the fracture energy of the material [6,7]. A strain softening law was implemented in the numerical model for simulating the tensile post-cracking behaviour of SFRC. This law was presented elsewhere [8].

Reinforced cracked concrete: A tension-stiffening model was developed for simulating the post-cracking behaviour of concrete (or SFRC) reinforced with conventional rebars. This model takes into account the main properties of the conventional reinforcement and the fracture parameters of the plain concrete (or SFRC). This model was described in another work [8].

Conventional reinforcement: Steel rebars are modelled using the laws proposed by Menegotto and Pinto [9].

Laminates of carbon fibre reinforced polymer: A linear stress-strain relationship was implemented for modelling the linear-elastic brittle behaviour of the CFRP laminates.

3 - Model appraisal

To assess the model performance, the design resistant moment of the slab cross section represented in Figure 5 will be determined and compared with the data furnished by the slab's supplier, included in Table 1.

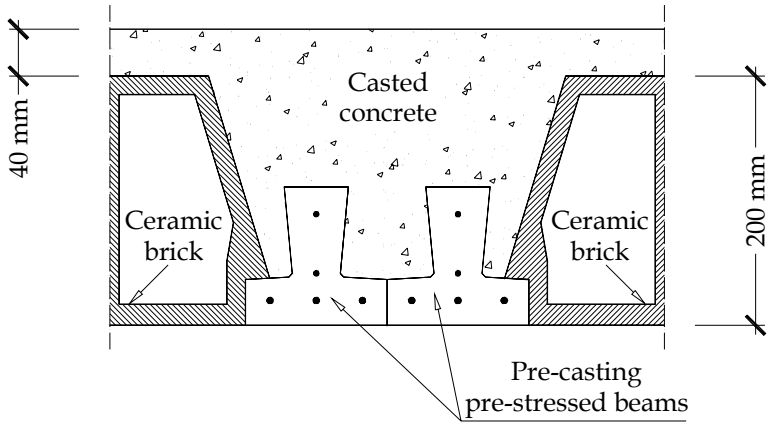

Figure 5 – A modulo of the slab.

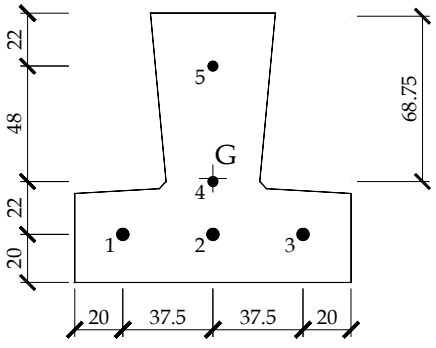

Figure 6 – Wires of the beams.

The slab is composed by pre-casting pre-stressed beams of C25/30 concrete and ceramic bricks. According to the slab supplier, the values on Table 1 were obtained considering a casted concrete of class C20/25. Table 2 includes the characteristics of the reinforcement on the pre-casting pre-stressed concrete beams (see also Figure 6).

Table 1 – Slab characteristics according to the supplier.

Slab reference	Thickness (mm)		Reference of the pre-stressed beam	Dead load (kN/m^2)	Limit states			
					Ultimate		Serviciability	
	Total	Above the brick			M_{Rd} (kNm/m)	V_{Rd} (kN/m)	M_{fctk} (kNm/m)	EI (kNm^2/m)
2S4-22B-24	240	40	S4	4.36	94.9	69.7	54.7	24075

Table 2 – Characteristics of the steel wires of the pre-casting pre-stressed concrete beams (see Fig. 6).

Wire number	Diameter (mm)	Pre-stress at long time (MPa)
1, 2 e 3	5.0	740
4	4.0	790
5	4.0	910

Figure 7 represents the cross-section approach adopted for design purposes. The corresponding four-nodded finite element mesh used is shown in Figure 8.

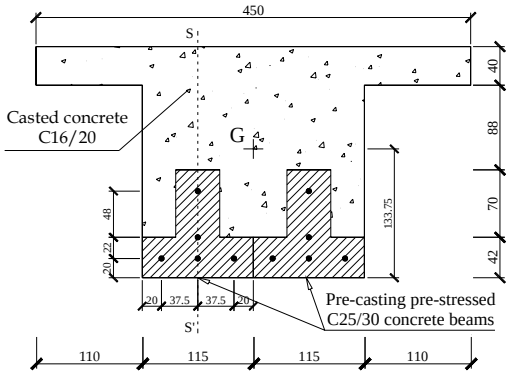

Figure 7 – Geometry assumed for the numerical simulation.

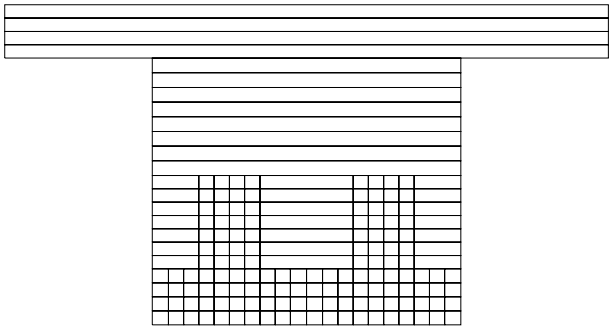

Figure 8 – Four-nodded finite element mesh.

The pre-stress on wires indicated on Table 2 introduces on the concrete pre-casting beams the stress field represented in Figure 9. To evaluate these stresses it was assumed a design compression strength of $0.85 \times f_{cd}$=14.2MPa (C25/30) for the concrete, and the finite element mesh represented in Figure 10. In the bottom surface the compression stress is about 10MPa, less than the concrete design compression strength.

To evaluate the compression strength of the casted concrete applied in the slab, six cylinder-drilled cores of 100mm diameter and 100mm length were tested in a compressive load frame. Using the recommendations proposed by ASTM [10] the average compression strength and the standard deviation were f_{cms}=27.4MPa and s_p=3.01MPa, respectively. To evaluate the characteristic and design values it was used the expression proposed by RILEM [11]

$$f_{ck} = f_{cms} - \frac{s_p\, t_{10}}{\sqrt{n}} - 1.645\, s_p \left(1 + \frac{s_p\, t_{10}}{f_{cms}\, \sqrt{n}} \right) \qquad (1)$$

where n is the number of specimens and t_{10} is the value for the "student distribution" at 10% fractile, which for n=6 is 1.48. Using these data it was obtained a f_{ck}=20.3MPa and a f_{cd}=13.5MPa, which corresponds to a C20/25 concrete class. However, taking into account that shrinkage cracks were observed in some drilled cores (see Figure 11) it was considered the C16/20 concrete class for design purposes. For the maximum compression strain allowed in concrete it was considered a value of 3.5‰, in agreement with the CEB-FIP Model Code.

Assuming the concrete of the pre-casting pre-stressed beams has the initial stress/strain field represented in Figure 9 and E_p=190GPa, f_{pud}=1715/1.15=1491MPa and $f_{p0.1d}$=1490/1.15=1296MPa for the design constitutive law of the steel wires, the moment-curvature relationship, represented in

Figure 12, was obtained, from which it can be concluded that the model estimates quite well the design resistant moment, M_{Rd}, given in the technical data of the slab's supplier (see Table 1). In all the numerical simulations it was neglected the concrete tensile contribution. The M_{Rd} value was conditioned by the maximum strain limit in the steel wires (see figure inset of Figure 12).

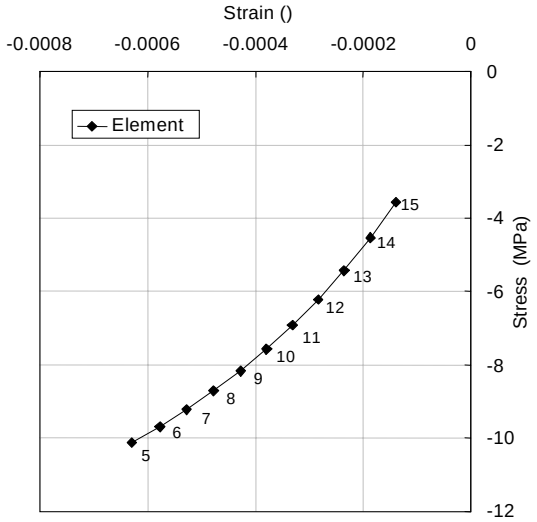

Figure 9 – Compression stress on concrete of the pre-casting pre-stressed beams.

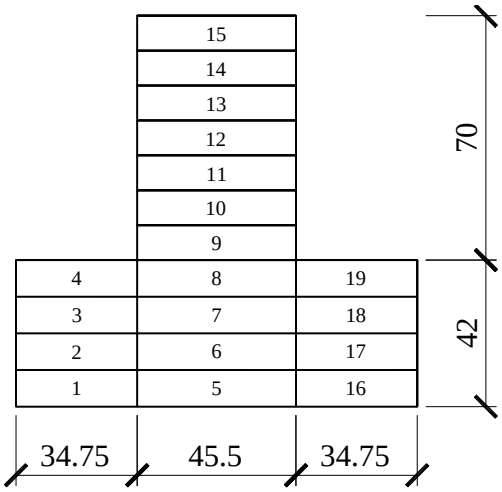

Figure 10 – Finite element mesh for the pre-casting pre-stressed beam.

Figure 11 – Some drilled cores had shrinkage cracks.

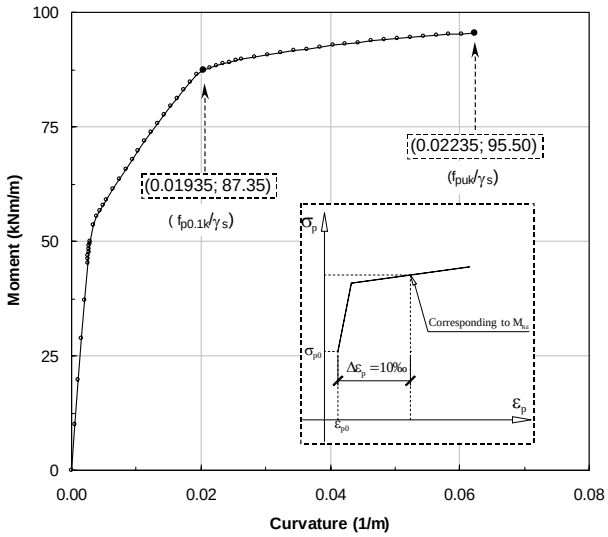

Figure 12 – Moment-curvature relationship for the slab.

4 – Numerical model applied for strengthening the slab

4.1 – Introduction

Any strengthening strategy will be applied when the slab is submitted to its dead load and to the revetments. For these loads the design moment (M_{Sd}) is 46kNm/m. Figure 13a illustrates the strains and the stresses in the slab cross-section for this loading regime. Figure 13b gives some support for understanding the stress path observed in the pre-casting pre-stressed concrete beams. For this purposed the layers 1 and 2 were considered. Under the pre-stress loading the stress in these layers is σ'_{C1} and σ'_{C2}, respectively (see Figure 13b). When the slab dead weight and the slab revetments are actuating, these two concrete layers unload, following the branches represented in Figure 13b. Since the

strain increment in layer 2 is higher than in layer 1, and the concrete tensile strength is neglected, the residual compression strength in layer 1, σ_{C1}, is higher than the stress in layer 2, σ_{C2}.

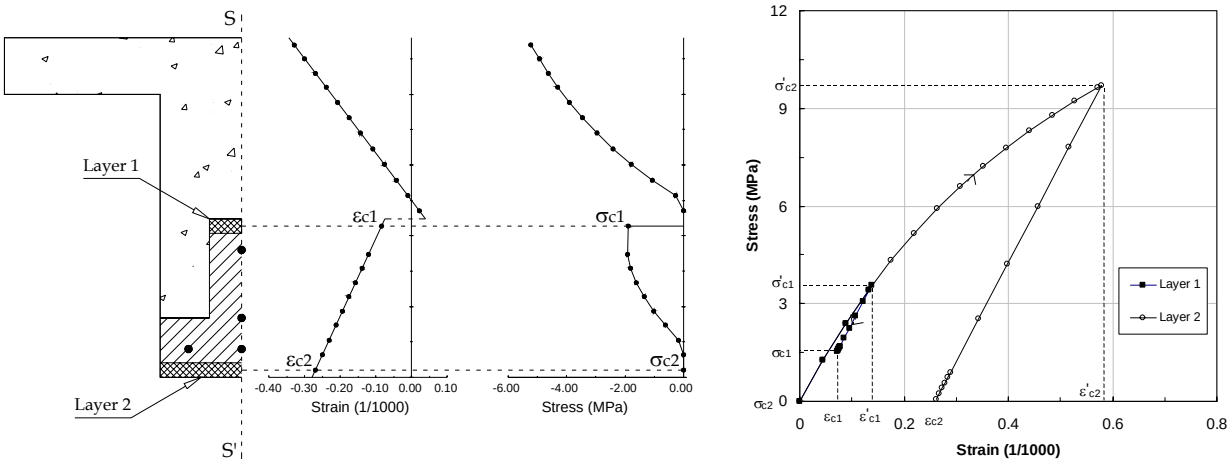

Figure 13 – Strain and stress field for the slab dead load and revetments.

4.2 – Using laminates of carbon fibre reinforced polymer (CFRP)

Comparatively to reinforcing traditional materials, the advanced composite materials have higher tensile strength, higher resistance to the environmental aggressiveness, are much more lightweight and more easy to apply. In some applications, the higher costs of the composite materials can be compensated by a significant decrease in the time spent on the strengthening procedures. Another important aspect is the marginal changing in the geometrical configuration of the element to be repaired when composite materials are used.

In the bottom surface of each pre-casting pre-stressed concrete beams a CFRP laminate of 50mm width and 1.2mm thick was glued using an epoxi compound. According to the technical data furnished by the supplier [12] the Young modulus and the tensile strength of the laminates proposed are E_L=150GPa and f_{uL}=2000MPa, respectively. To avoid the occurrence of the peeling phenomenon [13] in these composites, the design stress was limited to the half of its ultimate tensile strength. For the properties of the other materials it was used the values previously indicated. Figure 14 represents the moment-curvature relationship for the slab reinforced with CFRP laminates. The design resistant moment, M_{Rd}, is 111kNm/m, which is higher than the design moment of the loading actions (M_{Sd}=106kNm/m). The M_{Rd} value was conditioned by the concrete compression strain limit (3.5‰). For this M_{Rd} the stress in CFRP laminates is 616MPa (see Figure 15), which is less than the maximum allowed tensile stress ($f_{Ld}=f_{Lu}/2$) and the tensile stress in the highest strained steel wire is 1308MPa, less than the design ultimate stress (see Figure 16).

4.3 – Using a top overlayer of SFRC

The increase on the slab load bearing capacity provided by the previous strengthening strategy was limited by the allowed maximum concrete compression deformability. To retrieve the high tensile strength of the CFRP laminates without occurring the crushing of the casted concrete, a 30mm thick C20/25 SFRC top overlayer of 30 Kg/m^3 of Dramix ZP305 steel fibres [14] was applied. This SFRC layer was bonded to the casted concrete using metallic connectors fixed by an epoxy compound. These connectors were designed for resisting to the shear stresses between these two concrete layers. From Figure 14 it can be observed that the resistant moment is 112kNm/m, higher than the M_{sd}, and the response is much more ductile (see also Figure 17). This last observation can also be taken from the relationship between curvature and the compression stress at the SFRC top surface, illustrated in Figure 18. The M_{Rd} value was conditioned by the strain limit in the steel wires. A total strain of 13.9‰ ($\varepsilon_{po} + \Delta\varepsilon_p$ =3.9‰+10‰) was attained for M_{Rd}=112kNm/m, which corresponds to a stress of σ_p =1416MPa.

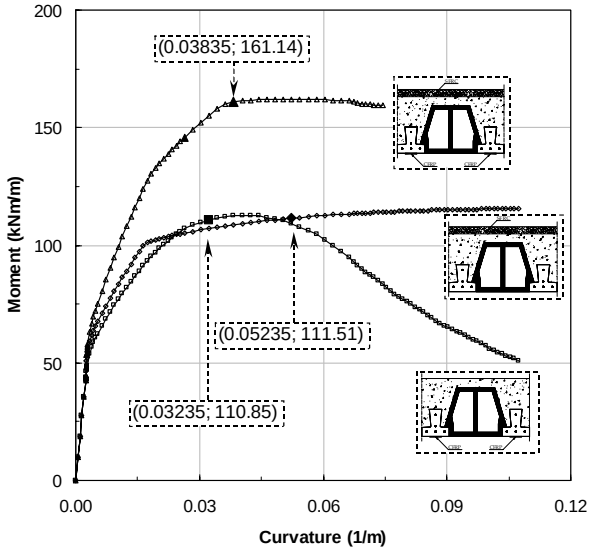

Figure 14 - Moment-curvature relationships for the reinforcing strategies.

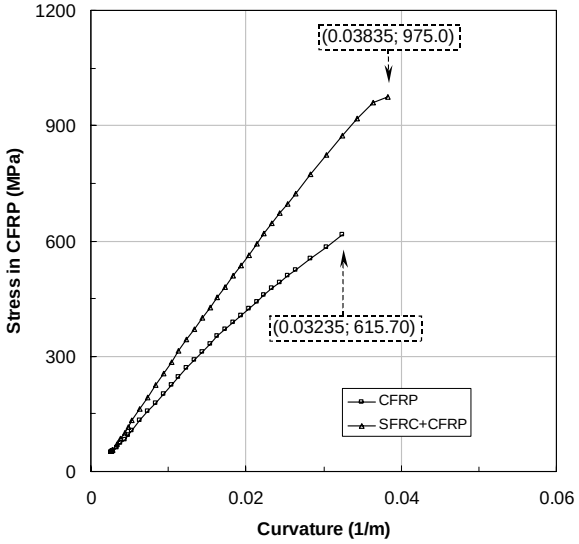

Figure 15 – Relationship between the stress in the CFRP laminates and the curvature.

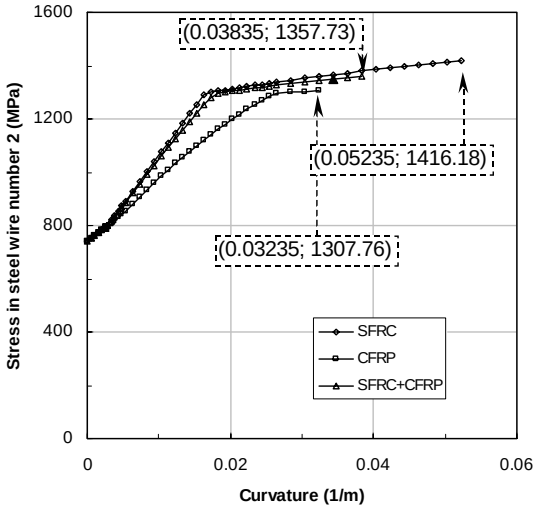

Figure 16 – Relationship between the stress in the highest strained wire and the curvature.

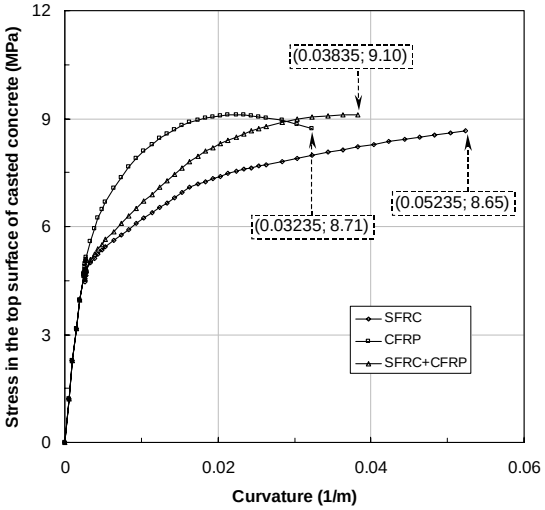

Figure 17 – Relationship between the curvature and the compression stress at the casted concrete top surface.

4.4 – Using CFRP and SFRC

Applying simultaneously CFRP laminates and a SFRC overlayer the ultimate moment is increased significantly (see Figure 14). The maximum moment was conditioned by the maximum stress allowed in CFRP laminates, but the compression strain limit at SFRC overlayer was almost attained (3.2‰), and the strain at top surface of the casted concrete is also significant (2.3‰), indicating that this strategy leads to a well profit of the all intervening materials.

5 – Conclusions

Three strengthening strategies for increasing the load bearing capacity of a concrete slab were analysed using a numerical model developed for this purpose. The first strategy was based on gluing CFRP laminates on the pre-casting pre-stressed C25/30 concrete beams. The design resistant moment (M_{Rd}) is 5% higher than the design loading moment (M_{Sd}), and its value is conditioned by the compression strain at the top surface of the casted concrete. In the second strategy a 30mm thick top overlayer of SFRC was applied. In this case the M_{Rd} is also 5% higher than the M_{Sd} but it is conditioned by the strain limit in the

wires, being the response much more ductile. The third strengthening strategy is a conjugation of the last two strategies, resulting a M_{Rd} 53% higher than the M_{Sd}, limited by the stress at CFRP laminates. For this M_{Rd}, the compression strain at top surface of the casted concrete and at top surface of the SFRC overlayer is near their limit values and the strain at the highest strained wire is a little bit above its limit, which indicates to be an effective reinforcing strategy. However, for the loads acting on the slab and taking into account economical reasons, the strategy based on SFRC overlayer was proposed to solve the problem. Figure 19 shows the aspect of the slab after to be strengthened.

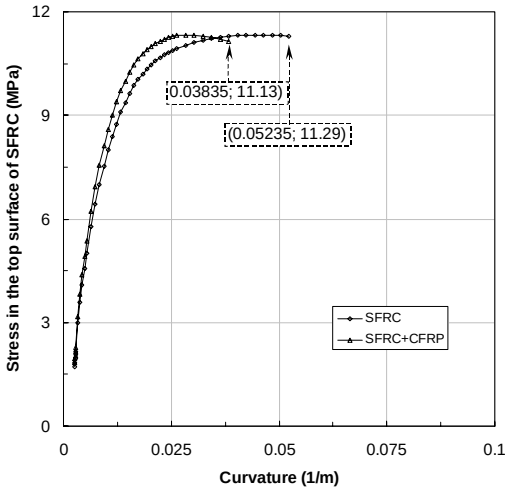

Figure 18 – Relationship between the curvature and the compression stress at SFRC top surface.

Figure 19 – View of the concrete slab after has been strengthened using a SFRC over-layer.

References

[1] – ACI 440R-96, "State-of-the-art report on fiber reinforced plastic reinforcement for concrete structures", *reported by ACI Committee 440, American Concrete Institute*, Farmington Hills, Michigan, 68 pp.

[2] – ACI 544.1R-96, "State-of-the-art report on fiber reinforced concrete", *ACI Manual of Concrete Practice – Part 5 – ACI International*, 1997, 66 pp.

[3] – CEB-FIP Model Code 1990. *Comite Euro-International du Beton*, Bulletin d'Information nº 213/214, Ed. Thomas Telford, (1993).

[4] – Scott, B.D.; Park, R.; Priestley, M. J. N. (1982), "*Stress-strain behavior of concrete confined by overlapping hoops at low and high strain rates*", Journal of the American Concrete Institute, January-February.

[5] – Thompson, K.J.; Park, R. (1980), "*Moment-curvature behaviour of cyclically loaded structural concrete members* ", Journal Structural Division, Proc. Inst. Civ. Engrs. Part 2, June, p.p. 317-341.

[6] – Barros, J.A.O., Figueiras, J.A. "Flexural behavior of steel fiber reinforced concrete: testing and modelling", Journal of Materials in Civil Engineering, ASCE, Vol. 11, Nº 4, pp 331-339, 1999.

[7] – Barros, J.A.O., Sena Cruz, J. "Fracture energy of steel fibre reinforced concrete", Journal of Mechanics of Composite Materials and Structures, Vol. 8, No. 1 pp.29-45, January-March 2001.

[8] – Barros, J.A.O., Figueiras, J.A. "Nonlinear analysis of steel fibre reinforced concrete slabs on grade", Computers & Structures, Vol.79, No.1, pp. 97-106, January 2001.

[9] – Menegotto, M.; Pinto, P. (1973), "*Method of analysis for cyclically loaded R.C. plane frames including changes in geometry and non-elastic behavior of elements under combined normal force and bending*", Symposium on Resistance and Ultimate Deformability os Structures Acted on by Well Defined Repeated Loads, IABS Reports Vol. 13, Lisbon.

[10] – ASTM Committee C-9, Subcommittee C09.61, "Standard test method for obtaining and testing drilled cores and sawed beams of concrete", ASTM, pp.24-27, 1990.

[11] – RILEM TC 162 – TDF, Materials and Structures, Vol. 33, pp 75-81, March 2000.

[12] – Technical data sheet of MBRACE Laminates, LM50×1.2, 2000.

[13] – Rostásy, F.S., "Assessment of the suitability of CRP plates from the S&P CRP system for use as adhesive-bonded reinforcement to strengthen concrete constructional elements and bases of assessment for their general approval by the construction supervisory authorities", expert opinion nº 98/0322, S&P Reinforcement, TU Braunschweig, 46 pp., 1998.

[14] – Technical data sheet of Dramix ZP305 steel fibres, N.V. Bekaert S.A., 1998.